Large-Amplitude Vibrations of Spring–Hinged Beams

G. Venkateswara Rao* and K. Kanaka Raju†
Vikram Sarabhai Space Center, Trivandrum 695 022, India

Nomenclature

a	=	maximum lateral displacement [Eqs. (5) and (6)]
b, c	=	constant [Eq. (5)]
E	=	Young's modulus
I	=	area moment of inertia
k	=	rotational spring stiffness
L	=	length of the beam
m	=	mass per unit length of the beam
P	=	tension in the beam due to large amplitudes
r	=	radius of gyration
T_{NL}	=	nonlinear period
t	=	time variable
$W(t)$	=	time function of lateral displacement
$w(x)$	=	spatial function of lateral displacement
x	=	axial coordinate
α	=	a/r
β	=	coefficients in Eqs. (8–10)
γ	=	rotational spring stiffness parameter (kL/EI)
λ_L	=	nondimensional frequency parameter ($m\omega_L^2 L^4/EI$)
ω_L	=	linear radian frequency
ω_{NL}	=	nonlinear radian frequency

Introduction

COMPONENTS such as uniform beams are encountered in many engineering structures including aerospace structures, such as framed interstages and payload adapters. These structures experience a severe dynamic environment during flight. Because these structural elements are slender, they are prone to large amplitudes. As such their frequency–amplitude relationship has to be evaluated. This is also useful for frequency-response analysis.

The first attempt to study the large-amplitude vibration behavior of hinged beam, with axially immovable ends is by Woinowsky-Krieger.[1] Some approximate analytical methods such as Ritz–Galerkin (see Ref. 2) and versatile numerical methods such as the finite element method (with some simplifying assumptions)[3,4] are used to solve this problem. A refined accurate finite element model is presented by Singh et al.[5] However, only classical boundary conditions are considered in these studies. Also, these methods[2–4] assume both spatial and temporal modes for the lateral displacement of the vibrating beam with large amplitudes.

In actual practice, depending on the end support flexibility, the ends of the beams can be treated as elastically restrained against rotation. As such, a study of the large-amplitude behavior of slender uniform beams, with axially immovable ends, is important. This can be achieved by assuming elastic rotational springs with specific values of rotational stiffness to represent the type of support. Even though the finite element method with simplifying assumptions has been effectively used[6] for this purpose, it involves a large computational effort because of the multiple parameters involved in the problem.

Received 7 March 2002; revision received 21 May 2002; accepted for publication 11 June 2002.

*Group Director, Structural Engineering Group; gv_rao@vssc.org.
†Head, Software Development Section, Structural Design and Analysis Division, Structural Engineering Group.

In this Note, a simple analytical method is presented to obtain the large-amplitude behavior of spring–hinged uniform beams that are symmetric with respect to the midpoint of the span of the beam. The admissible functions for the lateral displacement for the spring–hinged boundary conditions are evaluated following the method proposed by Elishakoff.[7] The final governing differential equation in time is solved by numerical integration to obtain the ratio of nonlinear to linear frequencies.

Formulation

The differential equation governing the spring–hinged beam (Fig. 1), with axially[1] immovable ends is

$$EIw^{\mathrm{IV}} = -m\ddot{w} + Pw'' \tag{1}$$

with the boundary conditions (considering the right half of the beam because of symmetry)

$$w(L/2) = 0 \tag{2}$$

$$EIw'' + kw' = 0 \tag{3}$$

at $x = L/2$. A variable separable solution for w is assumed as

$$w = W \cdot w(x) \tag{4}$$

where W is a function of time t only. An admissible function for $w(x)$ in space is assumed as

$$w(x) = a + bx^2 + cx^4 \tag{5}$$

When the boundary conditions [Eqs. (2) and (3)] are used, $w(x)$ can be obtained in terms of a as

$$w(x) = a\left[1 - \frac{(48+8\gamma)}{(10+\gamma)}\left(\frac{x}{L}\right)^2 + \frac{(32+16\gamma)}{(10+\gamma)}\left(\frac{x}{L}\right)^4\right] \tag{6}$$

The tension P developed in the beam because of large amplitudes is given by[1]

$$P = \frac{EI}{4Lr^2}\int_0^{L/2} [w'(x)]^2\,\mathrm{d}x \tag{7}$$

Substituting Eq. (6) in Eq. (1), and eliminating the space variable by using the Galerkin error-minimization method, we get the final differential equation in time as

$$L^4 m\ddot{W}/EI = \beta_a W + \beta_b \alpha^2 W^3 \tag{8}$$

where $\alpha = a/r$ and

$$\beta_a = \frac{504(2+\gamma)(12+\gamma)}{124+22\gamma+\gamma^2} \tag{9}$$

$$\beta_b = \frac{1024(102+18\gamma+\gamma^2)}{35(10+\gamma)^2(124+22\gamma+\gamma^2)} \tag{10}$$

Note that, in the preceding equations, the extreme cases of simply supported and clamped conditions are represented when $\gamma = 0$ and when $\gamma \to \infty$, respectively. Equation (8) is the famous Duffing's equation and can be solved either through elliptic integral functions of first kind or by a direct numerical integration method.

Even though the solution of Eq. (8) can be elegantly represented in the form of elliptic integral functions of first kind,[8] one has to resort to either a curve fitting or an interpolation method to get the values of the elliptic functions. For a given γ and α, in general, the integrals cannot be read directly from the elliptic integral function tables

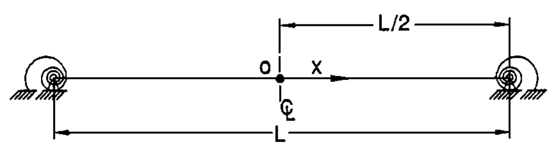

Fig. 1 Uniform spring–hinged beam.

because those are given for regular intervals, for example, in steps of 2-deg intervals.[9] Sometimes this process induces some errors in the numerical results. Hence, the direct numerical integration method, which will give the desired degree of accuracy, is used to obtain the numerical results for a given γ and α.

Direct Numerical Integration Method

Equation (8) can be written as

$$\ddot{W} + \beta_1 W + \beta_2 W^3 = 0 \tag{11}$$

where

$$\beta_1 = -(EI/mL^4)\beta_a \tag{12}$$

$$\beta_2 = -(EI/mL^4)\beta_b \tag{13}$$

When Eq. (11) is integrated, the nonlinear period $T_{\rm NL}$ can be obtained as

$$T_{\rm NL} = \frac{2\pi}{\omega_{\rm NL}} = 4\int_0^{\pi/2} \frac{d\theta}{\left\{\beta_1\left[1 + (\beta_2/2\beta_1)(1 + \sin^2\theta)a^2\right\}^{\frac{1}{2}}} \tag{14}$$

where $\omega_{\rm NL}$ is the nonlinear radian frequency. (The details of the algebraic manipulations are not given here because they are straightforward.)

The linear radian frequency ω_L can be easily obtained from Eq. (14) by neglecting the β_2 term, that is, $\beta_2 = 0$. The integral in Eq. (14) can be numerically integrated to obtain both ω_L for any γ and $\omega_{\rm NL}$ for any γ and α.

Numerical Results and Discussion

Figure 1 shows a uniform beam with ends hinged and also elastically restrained against rotation and symmetric about the center of the span of the beam. The accuracy of the present solution is thoroughly examined for $\gamma = 0$ (hinged beam) and for $\gamma = 10^5$ (modeling a clamped beam), which are the two extreme cases of the rotational spring stiffness parameter.

Table 1 gives the values of $\omega_{\rm NL}/\omega_L$ for a hinged beam ($\gamma = 0$) obtained from the present method along with literature values.[1–5] The value of the fundamental frequency parameter λ_L is also presented to assess the accuracy of the linear frequency obtained from the present solution. It can be seen from Table 1 that the present solution (the nonlinear part), with a simple polynomial approximation that includes γ, gives accurate results even for a very high α, for example, 5.0, and is very close to the exact solution of Woinowsky-Krieger[1] and the accurate solution obtained by the refined finite element method.[5]

The values of $\omega_{\rm NL}/\omega_L$ for a clamped beam ($\gamma = 10^5$ for the present solution) are tabulated in Table 2 along with the two finite element solutions[4,5] and with the solution obtained by Woinowsky-Krieger's[1] approach using a trigonometric admissible function for the spatial part of the lateral displacement $w(x)$, taken as $w(x) = (a/2)[1 - \cos(2\pi x/L)]$. Table 2 shows that the results (nonlinear part) obtained from the present solution match very well with the two finite element solutions.[4,5]

The results in terms of $\omega_{\rm NL}/\omega_L$ of a symmetric spring–hinged uniform beam can be seen in Table 3, for typical values of $\gamma = 1.0$ and 100.0. The present results (nonlinear part) agree well with the finite element solution of Rao et al.[4] for the available values of α. Furthermore, the authors are of the opinion that based on the accuracy achieved with the present solution for the extreme cases of $\gamma = 0$ and 10^5, the results obtained for the intermediate values of $\gamma = 1.0$ and 100.0 are more accurate compared to the finite element solution[4] with simplifying assumptions.

Table 1 Frequency ratio ($\omega_{\rm NL}/\omega_L$) values for a hinged beam ($\gamma = 0$)

α	Present solution[a]	Ref. 1	Ref. 2	Ref. 3	Ref. 4	Ref. 5
0.0	1.0000	1.0000	1.0000	1.0000	1.0000	1.0000
0.2	1.0038	1.0038	1.0037	1.0037	——	1.0037
0.4	1.0150	1.0150	0.0149	1.0148	——	1.0148
0.6	1.0333	1.0380	1.0330	1.0329	——	1.0331
0.8	1.0584	1.0580	1.0583	1.0578	——	1.0581
1.0	1.0897	1.0897	1.0897	1.0889	1.0888	1.0892
2.0	1.3196	1.3160	1.3220	1.3183	1.3110	1.3178
3.0	1.6290	1.6260	1.6370	1.6260	1.6022	1.6257
4.0	1.9808	1.9760	2.0000	1.9715	——	1.9761
5.0	2.3564	2.3500	2.3850	2.3341	——	2.3502

[a]Parameter $\lambda_L = 97.548$.

Table 2 Frequency ratio ($\omega_{\rm NL}/\omega_L$) values for a clamped beam ($\gamma = 10^5$)

α	Present solution[a]	Ref. 4	Ref. 5	Ref. 1 procedure[b]
0.0	1.0000	1.0000	1.0000	1.0000
0.2	1.0009	——	1.0009	1.0009
0.4	1.0035	——	1.0036	1.0037
0.6	1.0078	——	1.0080	1.0084
0.8	1.0138	——	1.0142	1.0149
1.0	1.0215	1.0217	1.0221	1.0231
2.0	1.0831	1.0831	1.0854	1.0892
3.0	1.1778	1.1756	1.1825	1.1902
4.0	1.2979	——	1.3055	1.3178
5.0	1.4369	——	1.4474	1.4647

[a]Parameter $\lambda_L = 503.96$. [b]With $w(x) = (a/2)[1 - \cos(2\pi x/L)]$.

Table 3 Frequency ratio ($\omega_{\rm NL}/\omega_L$) values of beam for $\gamma = 1.0$ and 100.0

α	$\omega_{\rm NL}/\omega_L$ Present solution	Ref. 6
	$\gamma = 1.0$[a]	
0.0	1.0000	1.0000
1.0	1.0651	1.0615
2.0	1.2379	1.2241
3.0	1.4791	1.4476
4.0	1.7603	——
5.0	2.0655	——
	$\gamma = 100.0$[b]	
0.0	1.0000	1.0000
1.0	1.0220	1.0218
2.0	1.0850	1.0835
3.0	1.1818	1.1764
4.0	1.3044	——
5.0	1.4459	——

[a]For the present solution, $\lambda_L = 133.71$, and for the solution of Ref. 6, $\lambda_L = 133.44$.
[b]For the present solution, $\lambda_L = 467.19$, and for the solution of Ref. 6, $\lambda_L = 464.05$.

Conclusions

A direct numerical integration method is used to evaluate the nonlinear vibration behavior of beams with symmetrically placed spring–hinges. The admissible lateral displacement function to satisfy the spring–hinged boundary conditions is derived in an elegant way. The numerical results presented indicate the efficacy of the method used to obtain the admissible lateral displacement functions to represent the spring–hinged boundary conditions. A thorough examination of the numerical results obtained from the present method when compared to those reported in literature demonstrates the accuracy that is achieved. To the best of the authors' knowledge, these are the accurate numerical results, presented for the first time, for the nonlinear vibrations of spring–hinged uniform beams.

Acknowledgment

The authors wish to thank B. Nageswara Rao, Structural Engineering Group, Vikram Sarabhai Space Center, for the useful discussions they had with him about the elliptic integral functions.

References

[1]Woinowsky-Krieger, S., "The Effect of an Axial Force on the Vibration of Hinged Bars," *Journal of Applied Mechanics*, Vol. 17, 1950, pp. 35–36.

[2]Srinivasan, A. V., "Large Amplitude Free Oscillations of Beams and Plates," *AIAA Journal*, Vol. 3, No. 10, 1965, pp. 1951–1953.

[3]Mei, C., "Nonlinear Vibrations of Beams by Matrix Displacement Method," *AIAA Journal*, Vol. 10, No. 3, 1972, pp. 355–357.

[4]Rao, G. V., Raju, K. K., and Raju, I. S., "Finite Element Formulation for the Large Amplitude Free Vibrations of Slender Beams and Orthotropic Circular Plates," *Computers and Structures*, Vol. 6, No. 3, 1976, pp. 169–172.

[5]Singh, G., Rao, G. V., and Iyengar, N. G. R., "Reinvestigation of Large Amplitude Free Vibrations of Beams Using Finite Elements," *Journal of Sound and Vibration*, Vol. 143, No. 2, 1990, pp. 351–355.

[6]Rao, G. V., and Raju, K. K., "Large Amplitude Vibrations of Beams with Elastically Restrained Ends," *Journal of Sound and Vibration*, Vol. 57, No. 2, 1978, pp. 302–304.

[7]Elishakoff, I., "Apparently First Closed-Form Solution for Frequency of Beam with Rotational Spring," *AIAA Journal*, Vol. 39, No. 1, 2001, pp. 183–186.

[8]Sathyamoorthy, M., *Nonlinear Analysis of Structures*, CRC Mechanical Engineering Series, CRC Press, Boca Raton, FL, 1998, pp. 26–38.

[9]Abramowitz, M., and Stegun, I. A., *Handbook of Mathematical Functions with Formulas, Graphs and Mathematical Tables*, National Bureau of Standards, Applied Mathematics Series 55, U.S. Dept. of Commerce, 1972, pp. 614, 615.

A. Berman
Associate Editor

Material Property Identification of Composite Plates Using Neural Network and Evolution Algorithm

Byung Joon Sung,* Jin Woo Park,* and Yong Hyup Kim†
Seoul National University,
Seoul 151-742, Republic of Korea

I. Introduction

THE baseline material properties of composite materials are susceptible to errors due to various defects during the manufacturing and operation. Thus, accurate estimation of the actual material properties is absolutely necessary for accurate numerical analysis. In the present Note, an efficient and accurate procedure is presented for the nondestructive material property identification of composite plates.

One of the popular nondestructive tests to identify material properties of composite structures is to utilize dynamic responses such as natural frequencies and mode shapes. Dynamics updating problems are solved by inverse procedures,[1–6] where perturbation methods based on the Taylor series expansion is usually adopted. Optimization techniques based on the conjugate-gradient method have been introduced that minimize the error norm of measured data and numerical results.[5] However, because the mass matrix is not updated, the material properties may be distorted due to the inaccuracies in the mass matrix.[6] Although the accuracy of the predicted dynamic behaviors may be enhanced by considering the dynamic response data, the evaluated static behavior is prone to error. With inclusion of static data in the update process, these difficulties could be relieved.[7]

Recently neural networks have drawn attention due to their powerful capabilities of pattern recognition, classification, and function approximation. A neural network has been utilized for the identification of material properties and damage detection by recognizing patterns of dynamic behavior and modal parameters.[8] Because the neural network does not require an explicit equation relating input data and output results, it can be utilized to solve complex inverse problems without calculation of the sensitivity, where the influence of certain parameters on the mass and stiffness of the structures is not obvious. Accurate prediction with neural networks usually requires many training input/output patterns, resulting in a large amount of computing time. This is one of reasons why most research is limited in application of neural network to simple problems.

In this Note, a neural network and an evolution algorithm are combined for the efficient prediction of material properties of structures. The neural network can make accurate predictions by using a small number of training data sets that is carefully selected through the evolution process.[9] The present method is a simple algorithm, shows rapid convergence, and does not require sensitivity computations. The applicability of the proposed method for the identification of the material properties of composite plates and the accuracy of the numerical analysis of static and dynamic behaviors using the identified material properties are investigated. The identification of material properties is accomplished by minimizing the difference between experimental measurements and the corresponding values of the dynamic responses and the static deflection obtained by the finite element analysis. The measurements of both static and dynamic responses ensure reliability in the prediction of the static as well as dynamic behavior. Accuracy and applicability of the present method are demonstrated by both numerical and experimental tests of carbon-fabric composite plates.

II. Optimization Using Neural Network and Evolution Algorithm

In the present study, the neural network, combined with the evolution algorithm, is used for the identification of material properties of composite structures. The neural network plays the role of approximating and recognizing the complex relationship between input patterns and output patterns. Figure 1 shows the prediction using the neural network. The input patterns consist of natural frequencies and static deflection, whereas the output patterns consist of the normalized material properties of the composite structures. The training input/output pairs are generated by finite element analysis of the composite structure. However, to obtain an accurate neural network prediction, a large amount of training data is required. The computational costs to generate such large training patterns and to train such large patterns would be very expensive. Therefore, in this work, we introduce an evolutionary procedure, where qualified training data are chosen for the neural network using a simple evolution algorithm. With such an evolutionary procedure, computational costs in training the neural network, as well as in generating the training patterns, can be substantially reduced.

An evolution algorithm is employed to aid in acceleration of the convergence of the neural network learning and in enhancement of the accuracy of the identified material properties. The criterion for the selection process is to minimize the error norm given as follows:

$$E = \left[\sum_i \left(\frac{w_i - w_i^0}{w_i^0} \right)^2 - \left(\frac{\delta - \delta^0}{\delta^0} \right)^2 \right]^{0.5} \tag{1}$$

where w_i and w_i^0 are the eigenvalues of the dynamic problem obtained numerically and experimentally, respectively, and δ and δ^0 are the numerical and experimental deflections, respectively. The scheme of optimization is shown in Fig. 2.

III. Identification Procedure

A schematic flowchart of the procedure is given in Fig. 2. The identification procedure is composed of the following processes.

First, k input/output pairs are generated for the initial neural network training. Note that k sets of initial vectors $\boldsymbol{X}_i$, $i = 1, \ldots, k$, are chosen from $U(a, b)^n$ as the output vector of the neural network, where $\boldsymbol{X}_i$ is a random vector, whose components are the normalized material properties. $U(a, b)^n$ denotes n-dimensional uniform distribution ranging over $[a, b]$. The corresponding input vector is the natural frequencies w_i and the static deflection δ obtained by the finite element method using the material properties of $\boldsymbol{X}_i$.

Second, material property is predicted using the neural network. The neural network trained by the k input/output patterns predicts

Received 13 February 2000; revision received 30 January 2002; accepted for publication 21 May 2002.

*Research Assistant, Department of Aerospace Engineering.

†Associate Professor, Department of Aerospace Engineering, Institute of Advanced Aerospace Technology; yhkim@gong.snu.ac.kr. Member AIAA.